

Local renal circadian clocks control fluid-electrolyte homeostasis and blood pressure

Natsuko Tokonami¹, David Mordasini^{1,6}, Sylvain Pradervand², Gabriel Centeno¹, Céline Jouffe^{1,5}, Marc Maillard³, Olivier Bonny^{1,3}, Frédéric Gachon^{1,5}, R. Ariel Gomez⁴, Maria Luisa S. Sequeira-Lopez⁴ and Dmitri Firsov^{1#}

¹ - Department of Pharmacology and Toxicology, University of Lausanne, Switzerland

² - Genomic Technologies Facility, University of Lausanne, Switzerland

³ - Service of Nephrology, Department of Medicine, CHUV, Lausanne, Switzerland

⁴ - Department of Pediatrics, University of Virginia School of Medicine, Charlottesville, USA

⁵ - Nestlé Institute of Health Sciences, Lausanne, Switzerland

⁶ - present address: Department of Nephrology and Hypertension, Inselspital, Bern, Switzerland

- to whom correspondence should be addressed:

Dmitri Firsov, Department of Pharmacology and Toxicology, University of Lausanne, 27 rue du Bugnon, 1005 Lausanne, Switzerland. e-mail: dmitri.firsov@unil.ch

running title: circadian clocks in the kidney

key words: circadian clocks, renin-angiotensin-aldosterone system, kidney, blood pressure, homeostasis.

Word count for abstract: 185

Word count for text: 3142

The circadian timing system is critically involved in the maintenance of fluid and electrolyte balance, and in blood pressure control. However, the role of peripheral circadian clocks in these homeostatic mechanisms remains unknown. We addressed this question in a mouse model carrying a conditional allele of the circadian clock gene *Bmal1* and expressing the Cre recombinase under the endogenous promoter of the *Renin* gene (*Bmal1^{lox/lox}/Ren1^dCre* mice). Analysis of *Bmal1^{lox/lox}/Ren1^dCre* mice showed that the floxed *Bmal1* allele was excised in the kidney. In the kidney, the BMAL1 protein expression was absent in the renin-secreting granular cells of the juxtaglomerular apparatus and in the collecting duct. A partial reduction of BMAL1 expression was observed in the medullary thick ascending limb. Functional analyses demonstrated that *Bmal1^{lox/lox}/Ren1^dCre* mice exhibit multiple abnormalities including an increased urine volume, changes in the circadian rhythm of urinary sodium excretion, an increased glomerular filtration rate (GFR) and a significant reduction in plasma aldosterone levels. These changes were accompanied by a reduction in blood pressure. These results show for the first time that local renal circadian clocks control body fluid and blood pressure homeostasis.

Circadian rhythmicity is a feature of a wide variety of physiological functions. Many of the functional rhythms are driven by the circadian timing system, a complex mechanism which coordinates all major cellular processes with geophysical time. It is thought that this coordination allows for the anticipatory adaptation of cells and tissues to the circadian changes in functional requirements. The circadian timing system is organized in a hierarchical manner. The masterclock of the system is located in the suprachiasmatic nucleus (SCN) of the hypothalamus and is synchronized to the daily light/dark cycle through the retino-hypothalamic tract. The peripheral circadian clocks, which are present in virtually all peripheral tissues, are synchronized to geophysical time through a wide range of masterclock-dependent stimuli, many of which remain unknown (reviewed in ¹). It is important to note, however, that despite the hierarchical structure of the circadian timing system and its continuous resetting by environmental time-cues, the intrinsic activity of both central and peripheral circadian clocks is largely self-sustained. On the molecular level, the masterclock and peripheral clocks share similar machinery based on transcriptional/translational feedback loops involving transcriptional activators BMAL1, CLOCK and NPAS2 and their own repressors PER1, PER2 and CRY1, CRY2 (reviewed in ²).

The circadian timing system is critically involved in the maintenance of fluid and electrolyte balance, and in blood pressure (BP) control. In mice, whole-body genetic inactivation of any of the circadian clock transcriptional activators or repressors leads to either increased or decreased BP ³⁻⁶ (reviewed in ⁷). In *clock*^{-/-} mice, the decrease in BP is accompanied by deep changes in circadian rhythms of urinary sodium and potassium excretion, loss of the circadian rhythmicity of plasma aldosterone levels and significant modifications in expression patterns of a great number of renal transcripts involved in different homeostatic functions ⁸. Doi et al. have shown that *Cry1/Cry2* double knockout mice exhibit significantly increased plasma aldosterone levels resulting in salt-sensitive

hypertension⁹. In humans, long-term misalignment of intrinsic circadian rhythms with geophysical time (e.g. shift-work) is increasingly recognized as a risk factor for the development of hypertension and progression of chronic kidney disease^{10, 11}. In genetic studies, Woon et al. have identified several polymorphisms in the promoter region of the human *Bmal1* gene that are associated with hypertension¹². However, to what extent the pathogenesis of these disorders is caused by the defect in the masterclock and/or in the local circadian clocks in different peripheral tissues remains unknown.

Here, we studied the role of peripheral circadian clocks in the maintenance of homeostasis of extracellular fluids and in BP regulation in a mouse model carrying a conditional allele of the circadian clock gene *Bmal1* and expressing Cre recombinase under the endogenous promoter of the *Renin* gene (*Bmal1*^{lox/lox}/*Ren1*^{dCre} mice)^{13, 14}. This mouse model was chosen because (i) the Renin-Angiotensin-Aldosterone System (RAAS) plays the central role in the regulation of BP, (ii) the activity of the RAAS exhibits significant circadian oscillations, and (iii) the inactivation of *Bmal1* results in the complete disruption of the molecular clock. Functional analysis revealed that *Bmal1*^{lox/lox}/*Ren1*^{dCre} mice exhibit multiple abnormalities, including defects in renal handling of sodium, water, calcium, magnesium and pH, significant changes in the circadian pattern of plasma aldosterone levels, an increase in the glomerular filtration rate (GFR) and a decrease in BP. These functional changes were accompanied by significant modifications in circadian patterns of mRNA expression of a number of renal transcripts involved in sodium, potassium and water balance. This study shows for the first time that local renal circadian clocks are indispensable for the maintenance of body fluid homeostasis and for BP control.

RESULTS

Inactivation pattern of Bmal1 in Bmal1^{lox/lox}/Ren1^dCre mice. The *Bmal1^{lox/lox}/Ren1^dCre* mice were generated by crossing mice bearing loxP sites flanking the exon 8 of the *Bmal1* gene with mice expressing Cre recombinase under the endogenous promoter of the *Renin-1d* (*Ren1^d*) gene. The *Bmal1^{lox/lox}/Ren1^dCre* mice were viable and did not show any obvious abnormalities when compared to *Ren1^dCre* mice used as controls (hereafter referred to as Control mice). As shown in Supplementary Figures 1A and 1B, they displayed a normal general motion activity and water-drinking behaviour, respectively. Gene expression analyses were performed at ZT0, the time of maximal expression of *Bmal1* mRNA^{15, 16}; the protein expression was quantified at ZT4 and/or ZT16, the time of expected maximal and minimal expression of BMAL1 protein, respectively (ZT- circadian or Zeitgeber time, where ZT0 is the time of light on and ZT12 is time of light off)¹⁷. The qPCR-based analysis of Cre mRNA levels in different tissues revealed highest expression in the kidney (Figure 1A). This correlated with the observation that the Cre-mediated excision of the floxed *Bmal1* allele was detectable only in the kidney, as demonstrated by RT-PCR analysis of total tissue RNA using primers flanking the floxed region (Figure 1B). Interestingly, the *Bmal1* mRNA levels were reduced not only in the kidney but also in the liver, thus suggesting that the circadian clock system in the liver is affected by the disruption of circadian clocks in renal cells (Figure 1C). However, immunohistochemistry showed that the vast majority of liver cells remained positive for *Bmal1* and, Western blotting did not reveal significant difference in BMAL1 protein expression between Control and *Bmal1^{lox/lox}/Ren1^dCre* mice (Supplementary Figures 2A and 2B, respectively (ZT4)).

Immunohistochemical analysis of Cre expression in the kidney (ZT4) showed that CRE protein is strongly expressed in the arterioles of juxtaglomerular apparatus but is also present in the cortical and medullary collecting duct (CCD and OMCD, respectively) and, at a

weaker level, in the medullary thick ascending limb (MTAL) (Figure 2 and Supplementary Figure 3; the Aquaporin-2 water channel was used as a marker of the principal cell of the CCD and OMCD, and Uromodulin was used as a marker of the thick ascending limb). The distribution of *Bmal1* mRNA and protein in kidneys of Control and *Bmal1*^{lox/lox}/*Ren1*^{dCre} mice was examined by qPCR performed on RNAs extracted from microdissected glomeruli or microdissected nephron segments, by Western probing of whole-cell lysates prepared from microdissected nephron segments (ZT4) and by immunohistochemistry (ZT4 and ZT16). As shown in Figure 3A, the *Bmal1* mRNA expression was markedly reduced in the CCD and OMCD. A partial reduction (~60%) in *Bmal1* mRNA expression was also observed in the MTAL. Importantly, the decrease in *Bmal1* mRNA expression correlated with the deletion of exon 8 of the *Bmal1* gene in the same nephron segments (Supplementary Figure 4). Western blot analysis revealed a parallel reduction of BMAL1 protein expression in the CCD, OMCD and MTAL (Figure 3B). Immunohistochemistry showed that BMAL1 protein is ubiquitously expressed in the kidney of Control mice but is absent in the juxtaglomerular cells (Supplementary Figures 5A (ZT4) and 5E, (ZT16)) and, in the CCD (Supplementary Figures 5B (ZT4) and 5F (ZT16)) and OMCD (Supplementary Figures 5C (ZT4) and 5G (ZT16)) of *Bmal1*^{lox/lox}/*Ren1*^{dCre} mice. The BMAL1 protein expression in the MTAL was significantly reduced, however a small population of MTAL cells exhibited positive staining for BMAL1 (Supplementary Figures 5D (ZT4) and 5H (ZT16)).

Function of the RAAS in Bmal1^{lox/lox}/Ren1^{dCre} mice. To assess the circadian pattern of the RAAS, mice were adapted to a 12-hour light/12-hour dark cycle (LD) for 2 weeks. Tissue and blood samples were collected from mice sacrificed every 4 hours over the course of circadian cycle. As shown in Figure 4A, kidneys from *Bmal1*^{lox/lox}/*Ren1*^{dCre} mice exhibited a moderate but significant reduction in *Ren1* mRNA expression (p=0.003, ANOVA, Supplementary Table 1). Western blot analysis revealed that renin protein levels follow a

circadian-like pattern in kidneys of Control mice with peak levels during the dark (activity) phase (Figures 4B and 4D). This pattern was disrupted in kidneys of *Bmall*^{lox/lox}/*Ren1*^dCre mice (Figures 4C and 4D, p=0.039, ANOVA, Supplementary Table 1). We also performed qPCR analysis of Cyclooxygenase-2 (*Cox-2*) and Peroxisome Proliferator-Activated Receptor Gamma (*Pparγ*), two genes that have been shown to be involved in the regulation of Renin synthesis and/or secretion. As shown in Supplementary Figures 6A and 6B, the expression patterns of both, *Cox-2* and *Pparγ*, were significantly changed in kidneys of *Bmall*^{lox/lox}/*Ren1*^dCre mice.

To assess the function of the RAAS, we examined circadian patterns of plasma Renin concentration (PRC) and plasma aldosterone concentrations in Control and *Bmall*^{lox/lox}/*Ren1*^dCre mice (Figure 5). As shown in Figures 5A and 5B, both the PRC and plasma aldosterone concentrations exhibited robust circadian rhythms (p<0.001, Supplementary Table 2; peak-to-trough amplitude in the circadian rhythm of PRC: 142.0% in Control mice, 70.4% in *Bmall*^{lox/lox}/*Ren1*^dCre mice; peak-to-trough amplitude in the circadian rhythm of plasma aldosterone concentration: 216.9% in Control mice, 117.8% in *Bmall*^{lox/lox}/*Ren1*^dCre mice). Interestingly, the plasma aldosterone concentration in Control (*Ren1*^dCre) mice follows a biphasic pattern, whereas previous studies in mice⁸, rats¹⁸ or humans¹⁹ have shown that plasma aldosterone concentration follows a bell-shaped circadian curve with a single peak at the time of transition between the inactive and active periods of the day. A possible explanation for this phenomenon is that the *Ren1*^dCre mice have a specific genetic background with only one copy of *Ren1*^d gene and one copy of *Ren2* gene.

Importantly, the circadian phases of PRC and plasma aldosterone concentrations were significantly different in both *Bmall*^{lox/lox}/*Ren1*^dCre and Control mice (PRC acrophases: ZT1 in Control mice and ZT22 in *Bmall*^{lox/lox}/*Ren1*^dCre mice; plasma aldosterone concentration acrophases: ZT9 in Control mice and ZT10 in *Bmall*^{lox/lox}/*Ren1*^dCre mice). ANOVA revealed

that the plasma aldosterone concentration was significantly reduced in *Bmal1*^{lox/lox}/*Ren1*^{dCre} mice (Figure 5B, $p < 0.001$; Supplementary Table 1), whereas the PRC was not different from Control mice ($p = 0.79$, Supplementary Table 1, Figure 5A). To address the difference in circadian phases between the PRC and plasma aldosterone concentration we examined the circadian pattern of plasma angiotensinogen levels. As shown in Figure 5C and Supplementary Table 2, the plasma angiotensin levels exhibited circadian pattern similar to that of plasma aldosterone levels with the maximal values in the second half of the light (inactivity) phase (plasma angiotensinogen levels acrophases: ZT8 in Control mice and ZT7 in *Bmal1*^{lox/lox}/*Ren1*^{dCre} mice; peak-to-trough amplitude in the circadian rhythm of plasma angiotensinogen levels: 44.7% in Control mice, 39.6% in *Bmal1*^{lox/lox}/*Ren1*^{dCre} mice). ANOVA revealed significant difference in plasma angiotensinogen levels between Control and *Bmal1*^{lox/lox}/*Ren1*^{dCre} mice ($p = 0.010$, Supplementary Table 1). This difference, while statistically significant, was slight in absolute terms. Statistical analysis with Student's t-test showed moderate difference in plasma aldosterone concentration, PRC and plasma angiotensinogen levels between Control and *Bmal1*^{lox/lox}/*Ren1*^{dCre} mice at several time-points of the circadian cycle.

*Urine and blood chemistry, renal function and blood pressure in *Bmal1*^{lox/lox}/*Ren1*^{dCre} mice.*

Analysis of 24-hour urine samples demonstrated that *Bmal1*^{lox/lox}/*Ren1*^{dCre} mice exhibit a mild increase in urinary volume, a decrease in urine osmolality and a tendency to hypercalciuria, hypermagnesuria and decreased urinary pH (Table 1). In plasma samples, a significant decrease in plasma osmolality and a tendency to hypochloremia were observed (Table 1). The glomerular filtration rate (GFR) measured at two circadian time-points (ZT6 and ZT18) was significantly increased in *Bmal1*^{lox/lox}/*Ren1*^{dCre} mice (Table 1). Of note, in both Control and *Bmal1*^{lox/lox}/*Ren1*^{dCre} mice, the GFR was significantly higher at ZT18 than

at ZT6 (Control mice: $p=0.002$; *Bmal1*^{lox/lox}/*Ren1*^dCre mice: $p<0.001$; unpaired Student's t-test).

To assess the circadian rhythms of urinary water, sodium and potassium excretion, urine was collected hourly from freely moving mice housed individually in metabolic cages. As shown in Figure 6A, there was no apparent difference in the circadian rhythms of urinary water excretion. The profiles of urinary sodium and potassium excretion were compared in the dark (activity) phase, where the accuracy of measurement is significantly higher due to higher volumes of collected urines. As shown in Figures 6B and 6C, the profile of urinary sodium but not potassium excretion was significantly different between Control and *Bmal1*^{lox/lox}/*Ren1*^dCre mice ($p<0.001$, interaction, Supplementary Table 1). This difference was also present, when the profiles of urinary sodium to potassium ratio were compared (Figure 6D and Supplementary Table 1). Circadian expression analysis of several genes involved in renal sodium, potassium and water handling (*α ENaC*, *NCC*, *Sgk1*, *ROMK*, *Aqp2*, *Aqp3*, *Aqp4* and *Avpr2*) revealed that all the selected genes, with the exception of *Avpr2*, exhibited a moderate but significant reduction in their mRNA expression levels at different time points of the circadian cycle (Supplementary Figure 7). The circadian analysis of plasma samples showed that both sodium and potassium levels exhibit circadian rhythms (Supplementary Table 2), however, there was no difference between Control and *Bmal1*^{lox/lox}/*Ren1*^dCre mice (Supplementary Figures 8A and 8B, respectively).

The BP was measured in conscious unrestrained mice using telemetry. As shown in Figure 7, both the systolic and diastolic BP were significantly decreased in *Bmal1*^{lox/lox}/*Ren1*^dCre mice (blood pressure recordings over 6 days are shown in the Supplementary Figure 9).

DISCUSSION

Accumulating evidence suggests that most, if not all, physiological functions are controlled by the circadian timing system. Although it is generally presumed that peripheral circadian clocks are involved in these regulatory mechanisms, there are only a limited number of studies that have addressed this question experimentally. For instance, Storch et al. have shown that the retinal intrinsic circadian clocks have a significant role in visual function¹⁴. Marcheva et al. have demonstrated that the inactivation of the circadian clock in pancreatic islets causes diabetes mellitus due to dysfunction of β -cells²⁰. In the kidney, the presence of the high amplitude circadian rhythms in the expression of the circadian clock genes has been evidenced in several studies^{8, 15, 16}. However, the functional role of the local renal circadian clocks has not been studied. To address this question, we crossed mice with floxed *Bmal1* gene with mice expressing the Cre recombinase under the endogenous promoter of the renin gene. The latter model has been widely used for the conditional inactivation of different genes expressed in the renin-secreting granular cells of the juxtaglomerular apparatus in the kidney²¹⁻²⁹. These studies showed that at the whole organ level the *Ren1^dCre* is strongly expressed in the kidney, whereas in other tested tissues the Cre expression was at or near background levels²⁴; *nota bene*: clearly, however, these results did not exclude that there might be minor populations of Cre-expressing cells in other tissues as well. These studies also demonstrated that within the kidney the Cre expression is not limited to the granular cells but is also present in the rest of the afferent arterioles, in the interlobular renal arteries and in the tubular segments¹³. For instance, Kurt et al. have demonstrated the presence of the CRE protein in the collecting duct²⁹. Here, we confirmed the tissue expression pattern of *Ren1^dCre* and demonstrated that in the kidney of *Bmal1^{lox/lox}/Ren1^dCre* mice the BMAL1 protein is absent in renin-secreting granular cells and in the CCD and OMCD. Surprisingly, we also found a significant reduction of BMAL1 protein levels in the MTAL. Since, to our knowledge, the expression of the renin gene in the thick ascending limb cells has not been reported, further

studies are needed to explain this finding. Collectively, these results suggest that (i) the *Bmal1* inactivation in *Bmal1^{lox/lox}/Ren1^dCre* mice is largely kidney-specific and, (ii) within the kidney, the inactivation of the circadian clock mechanism occurs in subpopulations of both vascular and tubular epithelial cells.

Functional analysis of *Bmal1^{lox/lox}/Ren1^dCre* mice has shown that the local renal circadian clocks are involved in a wide variety of specific homeostatic functions, including the maintenance of sodium, water, calcium, magnesium, chloride and pH balance. Interestingly, the phenotype of *Bmal1^{lox/lox}/Ren1^dCre* mice is quite similar to that observed in the total (whole-body) knockout of *Clock* (*clock^{-/-}* mice)^{8, 15}. The common features include mild polyuria, changes in the circadian pattern of urinary sodium excretion, a significant decrease in plasma aldosterone levels and low BP. Both models also display a circadian time point-dependent reduction in expression levels of several transcripts involved in water and sodium balance (*Aqp2*, *Aqp4*, *α ENaC* and *Sgk1*). These similarities suggest that, at least in part, the phenotype of *clock^{-/-}* mice has a renal origin.

Analysis of the renin-angiotensin-aldosterone axis revealed that *Bmal1^{lox/lox}/Ren1^dCre* mice exhibit significant changes in circadian patterns of renin protein and mRNA expression levels in the kidney. However, these changes did not result in the alteration of the PRC. Hence, these results indicate that factors other than renin are responsible for the decreased plasma aldosterone levels and low BP in *Bmal1^{lox/lox}/Ren1^dCre* mice. A surprising finding of our study is that the circadian rhythms of the PRC and plasma aldosterone concentration display nearly opposite circadian phases in both Control and *Bmal1^{lox/lox}/Ren1^dCre* mice. The circadian pattern of plasma aldosterone concentration in mice has been examined in several studies and all of them demonstrated the existence of a robust circadian rhythm that reaches its maximum at the time of transition between the light and dark phases^{8, 9}. The circadian variability in PRA and/or PRC has been shown in rats³⁰, humans³¹ and dogs³². To our

knowledge our study is the first to report the circadian pattern of the PRC in mice which exhibits its maximum at the time of transition between the dark and light phases. These results suggest a provocative hypothesis that circadian rhythmicity in plasma aldosterone concentrations and, potentially, in BP in mice is determined by the circadian rhythms in plasma angiotensinogen levels and not by the rhythmicity in available renin. To some extent this hypothesis is supported by the study of Kim et al, who demonstrated by using angiotensinogen gene titration in mice that differences in hepatic angiotensinogen mRNA expression were positively correlated with the expression of aldosterone synthase in adrenal glands and negatively correlated with renin expression in the kidney³³. Alternatively, these findings may suggest that circadian rhythmicity in plasma aldosterone concentrations in mice is mostly determined by the circadian clock-driven mechanisms in adrenal glands⁹.

An intriguing phenotype of *Bmal1*^{lox/lox}/*Ren1*^dCre mice is glomerular hyperfiltration which is not associated with proteinuria or glucosuria. Since the major mechanism of hyperfiltration is the reduction in the vascular resistance of the afferent arteriole, it is tempting to speculate that the circadian clock in the afferent arteriole has a direct effect on the afferent arteriole contractility. An increase in nitric oxide production in tubular cells is an alternative mechanism that could explain this phenomenon^{34, 35}.

Collectively, functional analysis of *Bmal1*^{lox/lox}/*Ren1*^dCre mice has shown that the local renal circadian clocks are involved in a variety of specific renal functions and in BP control. The specificity in establishing genotype-phenotype correlations in circadian clock-deficient models consists in the highly pleiotropic role of circadian clocks both on transcriptional/translational and functional levels. Indeed, recent estimates suggest that the circadian clock system controls thousands of genes in a cell-type dependent manner³⁶. Accordingly, it is not surprising that disruption of circadian clocks in renal cells results in a multitude of functional disturbances. In this study the circadian clock system was disrupted

only in a fraction of renal cell types, whereas the adult kidney is composed of more than 25 terminally differentiated cell types, each of which possesses its own circadian clock. Future studies are needed to fully explore the role of each of these clock systems in renal function.

CONCISE METHODS

Animals The procedures used to generate, and the characterization of *Bmal1*^{lox/lox} and *Ren1*^{dCre} mice described previously^{14, 17, 29, 37}. The *Bmal1*^{lox/lox} and *Ren1*^{dCre} mice were crossed in order to obtain *Bmal1*^{lox/+}/*Ren1*^{dCre} mice. The *Bmal1*^{lox/+}/*Ren1*^{dCre} mice were crossed with either *Bmal1*^{lox/lox} or *Bmal1*^{+/+} mice separately in order to obtain the *Bmal1*^{lox/lox}/*Ren1*^{dCre} and *Bmal1*^{+/+}/*Ren1*^{dCre} mice. 3-5 month old *Bmal1*^{lox/lox}/*Ren1*^{dCre} or *Ren1*^{dCre} (Control) male mice were used in all experiments. The animals were maintained *ad libitum* on the standard laboratory chow diet (KLIBA NAFAG diet 3800). Before all experiments, mice were adapted to a 12 hours light/ 12 hours dark (LD) cycle. All experiments with animals were performed in accordance with the Swiss guidelines for animal care, which conform to the National Institutes of Health animal care guidelines.

Antibodies Anti-Cre-recombinase antibody was from Novagen. Anti-BMAL1 antibody has been described elsewhere¹⁷. Anti-AQP2 and anti-GAPDH antibodies were from Santa Cruz, Anti-uromodulin antibody was from LS-Bio. Anti-actin antibody was from Sigma. Anti-Renin antibody was from Fitzgerald. Immunohistochemistry and Western blotting protocols are available in the Supplementary Methods.

Metabolic cages Mice were housed in individual metabolic cages (Tecniplast, Italy). Urine collection was performed after a 3-day adaptation period. Urine and blood chemistry was analyzed as previously described⁸. Hourly urine collection was performed as previously described⁸.

Blood levels of RAAS components Plasma renin concentration (PRC) was determined by radioimmunoassay (DPC) according to a previously published protocol³⁸. Angiotensinogen concentration was determined with mouse total angiotensinogen assay kit from IBL. Plasma aldosterone level was measured by radioimmunoassay (DPC).

Glomerular Filtration Rate (GFR) The GFR was determined according to the method described by Qi et al.³⁹.

Statistics Data are presented as mean \pm SEM or, as mean \pm SD, as indicated in the corresponding figure legends. The tests used include the 2-tailed, unpaired *t*-test and ANOVA. ANOVA were performed with genotype (Control, *Bmal1*^{lox/lox}/*Ren1*^{dCre}), time (ZT0, ZT4, ZT8, ZT12, ZT16 and ZT20) and interaction between time and genotype as factors. When possible, the mouse-to-mouse variability was taken into account by adding a factor for individual mice in the ANOVA model. *P* values are indicated in figure legends. A *P* value less than 0.05 was considered significant. Statistical analysis of circadian oscillations was performed as previously described¹⁵.

ACKNOWLEDGMENTS This work was supported by the Swiss National Science Foundation research grants 31003A-132496 (to D.F.) and by a grant from the Novartis Foundation (to D.F.)

STATEMENT OF COMPETING FINANCIAL INTEREST Authors have no competing interests to declare.

FIGURE LEGENDS

Figure 1. **A.** qPCR analysis of Cre mRNA expression (ZT0) in various tissues of Control (white bars) and *Bmal1*^{lox/lox}/*Ren1*^dCre (black bars) mice (see primer references in Supplementary Methods); data are means \pm SEM, n=5. **B.** RT-PCR analysis of *Bmal1* mRNA expression (ZT0) in different tissues of *Bmal1*^{lox/lox}/*Ren1*^dCre mice performed with primers flanking the floxed region. mRNA extracted from kidneys of whole-body (total) knockout of *Bmal1* was used as a control (see primer sequences in Supplementary Methods). **C.** qPCR analysis of *Bmal1* mRNA expression (ZT0) in various tissues of Control (white bars) and *Bmal1*^{lox/lox}/*Ren1*^dCre (black bars) mice (see primer references in Supplementary Methods); (n=5, data are means \pm SEM, n=5, * - p < 0.05, Student's t-test). Tissues were collected from mice sacrificed at ZT0 (**A**, **B** and **C**).

Figure 2. Immunohistochemical localization of Cre recombinase in the renal cortex (ZT4). Strong nuclear Cre staining (black) is present in the arterioles of juxtaglomerular apparatus (indicated with red arrows) and in the collecting duct (indicated with blue arrows), as evidenced by co-staining with aquaporin-2 water channel (red).

Figure 3. mRNA (**A**) and protein (**B**) expression of *Bmal1* in microdissected glomeruli (glom), proximal convoluted tubule (PCT), proximal straight tubule (PST), medullary thick ascending limb (MTAL), cortical thick ascending limb (CTAL), distal convoluted tubule (DCT), connecting tubule (CNT), cortical and outer medullary collecting duct (CCD and OMCD, respectively). Microdissection was performed at ZT4. Whole cell lysates of 20 mm microdissected nephron segments were used for Western blotting (**B**, n=3). **A:** data are means

± SEM, n=3, * - p<0.05, ** - p<0.01, *** - p<0.005; Student's t-test. Tissues were collected from mice sacrificed at ZT4.

Figure 4. Circadian patterns of renin mRNA and protein expression in Control and *Bmal1*^{lox/lox}/*Ren1*^dCre mice. **A.** Circadian pattern of renin mRNA expression in kidneys of Control (black line) and *Bmal1*^{lox/lox}/*Ren1*^dCre (red line) mice (n=6/time-point). Kidneys were extracted from mice sacrificed at indicated circadian time-points. Data are means ± SEM, n=6. Significant ANOVA factors: $P_{\text{genotype}}=0.003$, $P_{\text{time}}=0.013$. **B.** Circadian pattern of renin protein expression in kidneys of Control mice. This representative Western blot was performed on samples prepared by combining equivalent amounts of protein extracted from kidneys of six independent mice, in each time-point. **C.** Circadian pattern of renin protein expression in kidneys of *Bmal1*^{lox/lox}/*Ren1*^dCre mice. This representative Western blot was performed on samples prepared by combining equivalent amounts of protein extracted from kidneys of six independent mice in each time-point. **D.** Densitometry analysis of Western blots performed on individual samples of kidney protein extracts used in **B** (Control mice, black line) and **C** (*Bmal1*^{lox/lox}/*Ren1*^dCre mice, red line) (n=6/time-point). Data are means ± SEM, n=6, Significant ANOVA factors: $P_{\text{genotype}}=0.039$.

Figure 5. Circadian patterns of plasma renin concentration (PRC) (**A**), plasma aldosterone levels (**B**) and plasma angiotensinogen concentration (**C**) in Control (white bars) and *Bmal1*^{lox/lox}/*Ren1*^dCre (black bars) mice (n=10-12/time point). Data are means ± SEM (n=10-12, depending on time-point). Student's t-test significance: * - p<0.05, ** - p<0.01, *** - p<0.005. Significant ANOVA factors: $P_{\text{time}}<0.001$ (**A**); $P_{\text{genotype}}<0.001$, $P_{\text{time}}<0.001$, $P_{\text{interaction}}<0.001$ (**B**); $P_{\text{genotype}}=0.010$, $P_{\text{time}}<0.001$ (**C**).

Figure 6. Circadian patterns of urinary water (**A**), sodium (**B**) and potassium (**C**) excretion and urinary sodium to potassium ratios in Control (black line) and *Bmal1^{lox/lox}/Ren1^{dCre}* (red line) mice. Circadian pattern of urinary water excretion (**A**) was determined on the urine collected hourly over the 24-hour circadian cycle. The dynamics of urinary sodium and potassium excretion and of the sodium to potassium ratio (**B**, **C** and **D**, respectively) were determined on the urine collected hourly over the 12 hours of the activity phase of the circadian cycle (ZT12-ZT24). Data are means \pm SEM, n=21. Significant ANOVA factors: $P_{\text{time}} < 0.001$, $P_{\text{interaction}} < 0.001$ (**B**); $P_{\text{time}} = 0.010$ (**C**); $P_{\text{time}} < 0.001$, $P_{\text{interaction}} < 0.001$ (**D**).

Figure 7. Systolic (**A**) and diastolic (**B**) BP in Control (black line) and *Bmal1^{lox/lox}/Ren1^{dCre}* (red line) mice. For each mouse a mean of 6-day recording was calculated (the 6-day recordings are shown in Supplementary Figure 9); then, the mean of these values was determined for each genotype. Data are means \pm SEM, n=7 for both genotypes. Significant ANOVA factors: $P_{\text{time}} < 0.001$, $P_{\text{genotype}} < 0.001$ (**B**).

1. Saini, C, Suter, DM, Liani, A, Gos, P, Schibler, U: The mammalian circadian timing system: synchronization of peripheral clocks. *Cold Spring Harb Symp Quant Biol*, 76: 39-47, 2011
2. Bass, J: Circadian topology of metabolism. *Nature*, 491: 348-356, 2012
3. Curtis, AM, Cheng, Y, Kapoor, S, Reilly, D, Price, TS, Fitzgerald, GA: Circadian variation of blood pressure and the vascular response to asynchronous stress. *Proc Natl Acad Sci U S A*, 104: 3450-3455, 2007
4. Vukolic, A, Antic, V, Van Vliet, BN, Yang, Z, Albrecht, U, Montani, JP: Role of mutation of the circadian clock gene *Per2* in cardiovascular circadian rhythms. *Am J Physiol Regul Integr Comp Physiol*, 298: R627-634, 2010
5. Wang, Q, Maillard, M, Schibler, U, Burnier, M, Gachon, F: Cardiac hypertrophy, low blood pressure, and low aldosterone levels in mice devoid of the three circadian PAR bZip transcription factors DBP, HLF, and TEF. *Am J Physiol Regul Integr Comp Physiol*, 299: R1013-1019, 2010
6. Stow, LR, Richards, J, Cheng, KY, Lynch, IJ, Jeffers, LA, Greenlee, MM, Cain, BD, Wingo, CS, Gumz, ML: The circadian protein period 1 contributes to blood pressure control and coordinately regulates renal sodium transport genes. *Hypertension*, 59: 1151-1156, 2012
7. Firsov, D, Bonny, O: Circadian regulation of renal function. *Kidney Int*, 78: 640-645, 2010
8. Nikolaeva, S, Pradervand, S, Centeno, G, Zavadova, V, Tokonami, N, Maillard, M, Bonny, O, Firsov, D: The circadian clock modulates renal sodium handling. *J Am Soc Nephrol*, 23: 1019-1026, 2012
9. Doi, M, Takahashi, Y, Komatsu, R, Yamazaki, F, Yamada, H, Haraguchi, S, Emoto, N, Okuno, Y, Tsujimoto, G, Kanematsu, A, Ogawa, O, Todo, T, Tsutsui, K, van der Horst, GT, Okamura, H: Salt-sensitive hypertension in circadian clock-deficient *Cry*-null mice involves dysregulated adrenal *Hsd3b6*. *Nat Med*, 16: 67-74, 2009

10. Lieu, SJ, Curhan, GC, Schernhammer, ES, Forman, JP: Rotating night shift work and disparate hypertension risk in African-Americans. *J Hypertens*, 30: 61-66, 2012
11. Rubinstein, S, Wang, C, Qu, W: Occupational risk and chronic kidney disease: a population-based study in the United States adult population. *Int J Nephrol Renovasc Dis*, 6: 53-59, 2013
12. Woon, PY, Kaisaki, PJ, Braganca, J, Bihoreau, MT, Levy, JC, Farrall, M, Gauguier, D: Aryl hydrocarbon receptor nuclear translocator-like (BMAL1) is associated with susceptibility to hypertension and type 2 diabetes. *Proc Natl Acad Sci U S A*, 104: 14412-14417, 2007
13. Sequeira Lopez, ML, Pentz, ES, Nomasa, T, Smithies, O, Gomez, RA: Renin cells are precursors for multiple cell types that switch to the renin phenotype when homeostasis is threatened. *Dev Cell*, 6: 719-728, 2004
14. Storch, KF, Paz, C, Signorovitch, J, Raviola, E, Pawlyk, B, Li, T, Weitz, CJ: Intrinsic circadian clock of the mammalian retina: importance for retinal processing of visual information. *Cell*, 130: 730-741, 2007
15. Zuber, AM, Centeno, G, Pradervand, S, Nikolaeva, S, Maquelin, L, Cardinaux, L, Bonny, O, Firsov, D: Molecular clock is involved in predictive circadian adjustment of renal function. *Proc Natl Acad Sci U S A*, 106: 16523-16528, 2009
16. Gachon, F, Olela, FF, Schaad, O, Descombes, P, Schibler, U: The circadian PAR-domain basic leucine zipper transcription factors DBP, TEF, and HLF modulate basal and inducible xenobiotic detoxification. *Cell Metab*, 4: 25-36., 2006
17. Jouffe, C, Cretenet, G, Symul, L, Martin, E, Atger, F, Naef, F, Gachon, F: The circadian clock coordinates ribosome biogenesis. *PLoS Biol*, 11: e1001455, 2013
18. Gomez-Sanchez, C, Holland, OB, Higgins, JR, Kem, DC, Kaplan, NM: Circadian rhythms of serum renin activity and serum corticosterone, prolactin, and aldosterone concentrations in the male rat on normal and low-sodium diets. *Endocrinology*, 99: 567-572, 1976
19. Armbruster, H, Vetter, W, Uhlschmid, G, Zaruba, K, Beckerhoff, B, Nussberger, J, Vetter, H, Siegenthaler, W: Circadian rhythm of plasma renin activity and plasma aldosterone in normal man and in renal allograft recipients. *Proc Eur Dial Transplant Assoc*, 11: 268-276, 1975
20. Marcheva, B, Ramsey, KM, Buhr, ED, Kobayashi, Y, Su, H, Ko, CH, Ivanova, G, Omura, C, Mo, S, Vitaterna, MH, Lopez, JP, Philipson, LH, Bradfield, CA, Crosby, SD, JeBailey, L, Wang, X, Takahashi, JS, Bass, J: Disruption of the clock components CLOCK and BMAL1 leads to hypoinsulinaemia and diabetes. *Nature*, 466: 627-631, 2010
21. Gomez, RA, Pentz, ES, Jin, X, Cordaillat, M, Sequeira Lopez, ML: CBP and p300 are essential for renin cell identity and morphological integrity of the kidney. *Am J Physiol Heart Circ Physiol*, 296: H1255-1262, 2009
22. Neubauer, B, Machura, K, Chen, M, Weinstein, LS, Oppermann, M, Sequeira-Lopez, ML, Gomez, RA, Schnermann, J, Castrop, H, Kurtz, A, Wagner, C: Development of vascular renin expression in the kidney critically depends on the cyclic AMP pathway. *Am J Physiol Renal Physiol*, 296: F1006-1012, 2009
23. Sequeira-Lopez, ML, Weatherford, ET, Borges, GR, Monteagudo, MC, Pentz, ES, Harfe, BD, Carretero, O, Sigmund, CD, Gomez, RA: The microRNA-processing enzyme dicer maintains juxtaglomerular cells. *J Am Soc Nephrol*, 21: 460-467, 2010
24. Desch, M, Schreiber, A, Schweda, F, Madsen, K, Friis, UG, Weatherford, ET, Sigmund, CD, Sequeira Lopez, ML, Gomez, RA, Todorov, VT: Increased renin production in mice with deletion of peroxisome proliferator-activated receptor-gamma in juxtaglomerular cells. *Hypertension*, 55: 660-666, 2010
25. Chen, L, Faulhaber-Walter, R, Wen, Y, Huang, Y, Mizel, D, Chen, M, Sequeira Lopez, ML, Weinstein, LS, Gomez, RA, Briggs, JP, Schnermann, J: Renal failure in mice with Gsalpha deletion in juxtaglomerular cells. *Am J Nephrol*, 32: 83-94, 2010
26. Chen, L, Kim, SM, Eisner, C, Oppermann, M, Huang, Y, Mizel, D, Li, L, Chen, M, Sequeira Lopez, ML, Weinstein, LS, Gomez, RA, Schnermann, J, Briggs, JP: Stimulation of renin secretion by angiotensin II blockade is Gsalpha-dependent. *J Am Soc Nephrol*, 21: 986-992, 2010
27. Kurt, B, Kurtz, L, Sequeira-Lopez, ML, Gomez, RA, Willecke, K, Wagner, C, Kurtz, A: Reciprocal expression of connexin 40 and 45 during phenotypical changes in renin-secreting cells. *Am J Physiol Renal Physiol*, 300: F743-748, 2011
28. Castellanos Rivera, RM, Monteagudo, MC, Pentz, ES, Glenn, ST, Gross, KW, Carretero, O, Sequeira-Lopez, ML, Gomez, RA: Transcriptional regulator RBP-J regulates the number and plasticity of renin cells. *Physiol Genomics*, 43: 1021-1028, 2011
29. Kurt, B, Paliege, A, Willam, C, Schwarzensteiner, I, Schucht, K, Neymeyer, H, Sequeira-Lopez, ML, Bachmann, S, Gomez, RA, Eckardt, KU, Kurtz, A: Deletion of von Hippel-Lindau protein converts renin-producing cells into erythropoietin-producing cells. *J Am Soc Nephrol*, 24: 433-444, 2013
30. Rodriguez-Sargent, C, Cangiano, JL, Martinez-Maldonado, M: Circadian rhythms of plasma renin levels in the anesthetized rat. *Ren Physiol*, 5: 53-56, 1982

31. Williams, GH, Cain, JP, Dluhy, RG, Underwood, RH: Studies of the control of plasma aldosterone concentration in normal man. I. Response to posture, acute and chronic volume depletion, and sodium loading. *J Clin Invest*, 51: 1731-1742, 1972
32. Mochel, JP, Fink, M, Peyrou, M, Desevaux, C, Deurinck, M, Giraudel, JM, Danhof, M: Chronobiology of the renin-angiotensin-aldosterone system in dogs: relation to blood pressure and renal physiology. *Chronobiol Int*, 30: 1144-1159, 2013
33. Kim, HS, Lee, G, John, SW, Maeda, N, Smithies, O: Molecular phenotyping for analyzing subtle genetic effects in mice: application to an angiotensinogen gene titration. *Proc Natl Acad Sci U S A*, 99: 4602-4607, 2002
34. Anea, CB, Cheng, B, Sharma, S, Kumar, S, Caldwell, RW, Yao, L, Ali, MI, Merloiu, AM, Stepp, DW, Black, SM, Fulton, DJ, Rudic, RD: Increased superoxide and endothelial NO synthase uncoupling in blood vessels of Bmal1-knockout mice. *Circ Res*, 111: 1157-1165, 2012
35. Anea, CB, Zhang, M, Stepp, DW, Simkins, GB, Reed, G, Fulton, DJ, Rudic, RD: Vascular disease in mice with a dysfunctional circadian clock. *Circulation*, 119: 1510-1517, 2009
36. Koike, N, Yoo, SH, Huang, HC, Kumar, V, Lee, C, Kim, TK, Takahashi, JS: Transcriptional architecture and chromatin landscape of the core circadian clock in mammals. *Science*, 338: 349-354, 2012
37. Lopez, MLSS, Pentz, ES, Nomasa, T, Smithies, O, Gomez, RA: Renin cells are precursors for multiple cell types that switch to the renin phenotype when homeostasis is threatened. *Dev Cell*, 6: 719-728, 2004
38. Kim, SM, Mizel, D, Huang, YG, Briggs, JP, Schnermann, J: Adenosine as a mediator of macula densa-dependent inhibition of renin secretion. *Am J Physiol Renal Physiol*, 290: F1016-1023, 2006
39. Qi, Z, Whitt, I, Mehta, A, Jin, J, Zhao, M, Harris, RC, Fogo, AB, Breyer, MD: Serial determination of glomerular filtration rate in conscious mice using FITC-inulin clearance. *Am J Physiol Renal Physiol*, 286: F590-596, 2004

Table 1. 24h urine and plasma chemistry in Control and *Bmal1*^{lox/lox}/*Ren1*^dCre mice

	Control	<i>Bmal1</i> ^{lox/lox} / <i>Ren1</i> ^d Cre	p
Body weight (g)	26.7±3.4 (33)	26.5±2.4 (33)	NS
Urine			
Volume/g body weight (ml/g)	0.068±0.028 (33)	0.084±0.029 (33)	0.029
Osmolality (mosm/kg H ₂ O)	2937±605 (12)	2329±341 (12)	0.006
pH	6.29±0.17 (12)	6.11±0.23 (12)	0.050
UV*Na ⁺ /g body weight (μmol/g)	11.8±3.2 (12)	10.0±1.3 (12)	NS
UV*K ⁺ /g body weight (μmol/g)	32.8±7.3 (12)	29.6±3.2 (12)	NS
UV*Cl ⁻ /g body weight (μmol/g)	20.5±3.9 (12)	19.6±2.3 (12)	NS
UV*Ca ²⁺ /g body weight (μmol/g)	0.13±0.03 (12)	0.22±0.16 (12)	0.061
UV*Mg ²⁺ /g body weight (μmol/g)	2.17±0.50 (12)	2.67±0.70 (12)	0.059
UV*PO ₄ ³⁻ /g body weight (μmol/g)	5.08±1.68 (12)	5.80±1.96 (12)	NS
UV*Creatinine/g body wieight (μmol/g)	0.52±0.09 (12)	0.57±0.14 (12)	NS
UV*Urea/g body weight (μmol/g)	146.8±27.4 (12)	146.9±19.6 (12)	NS
UV*Urate/g body weight (μmol/g)	78.3±14.2 (12)	73.4±16.6 (12)	NS
UV*Glucose/g body weight (μmol/g)	0.21±0.03 (12)	0.29±0.18 (12)	NS
UV*Total protein/g body weight (mg/g)	0.65±0.09 (12)	0.48±0.20 (12)	0.011
Plasma			
Osmolality (mosm/kg H ₂ O)	311.1±6.0 (9)	305.1±3.6 (8)	0.026
Na ⁺ (mM)	158.2±0.7 (9)	157.2±0.9 (9)	NS
K ⁺ (mM)	4.68±0.10 (9)	4.74±0.16 (9)	NS
Cl ⁻ (mM)	122.4±3.0 (9)	110.0±2.1 (9)	0.071
Ca ²⁺ (mM)	2.12±0.10 (9)	2.07±0.05 (9)	NS
Mg ²⁺ (mM)	1.28±0.09 (9)	1.27±0.04 (9)	NS
Creatinine (μM)	15.1±2.0 (9)	15.9±3.0 (9)	NS
GFR			
GFR ZT6 (μl/min)	208.3±18.6 (6)	263.2±34.5 (5)	0.008
GFR ZT18 (μl/min)	322.9±19.1 (5)	386.9±25.2 (5)	0.002

Values are means ± SD. Student's t-test.

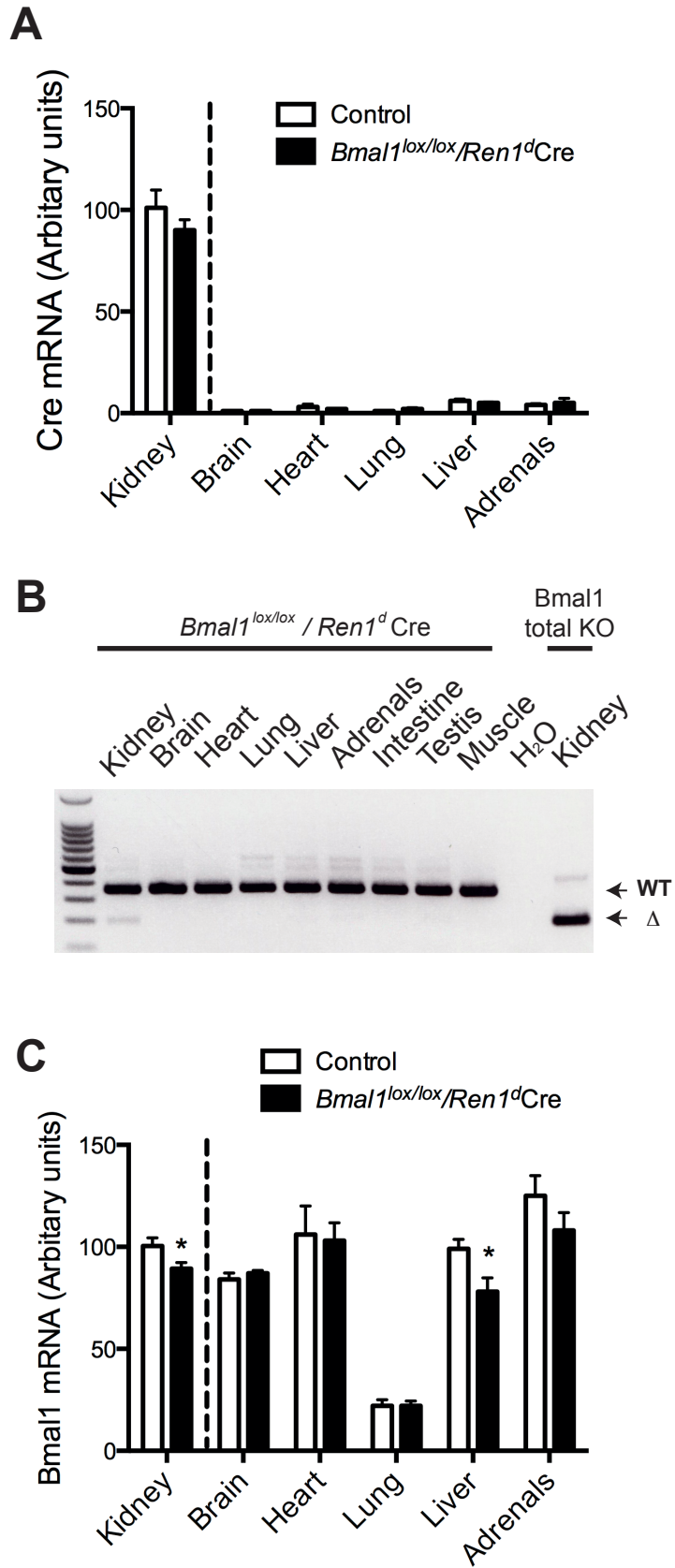


Figure 1, Tokonami et al.

Cre / AQP2

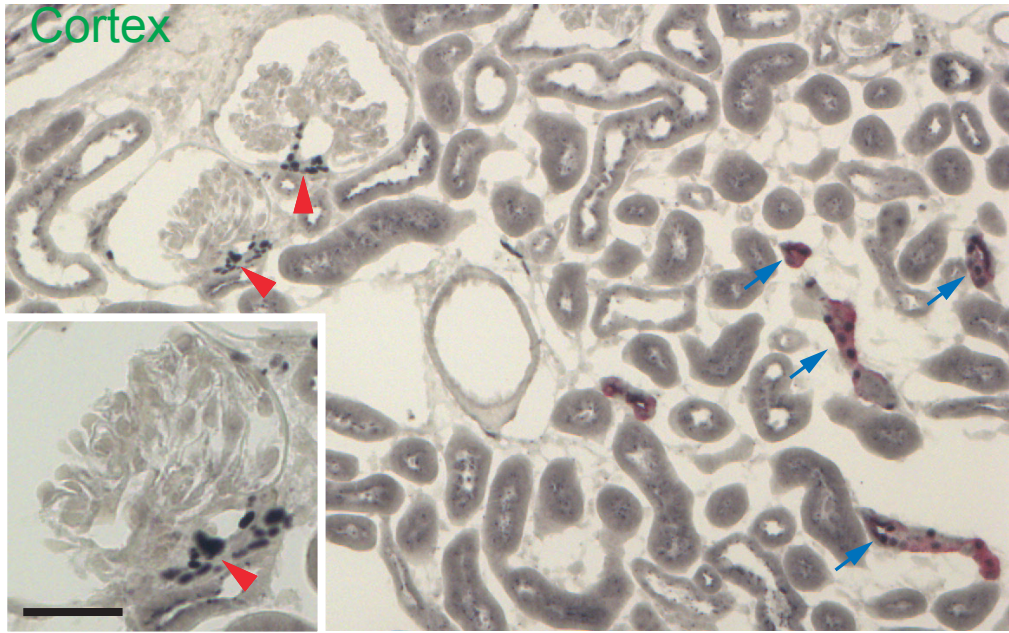


Figure 2, Tokonami et al.

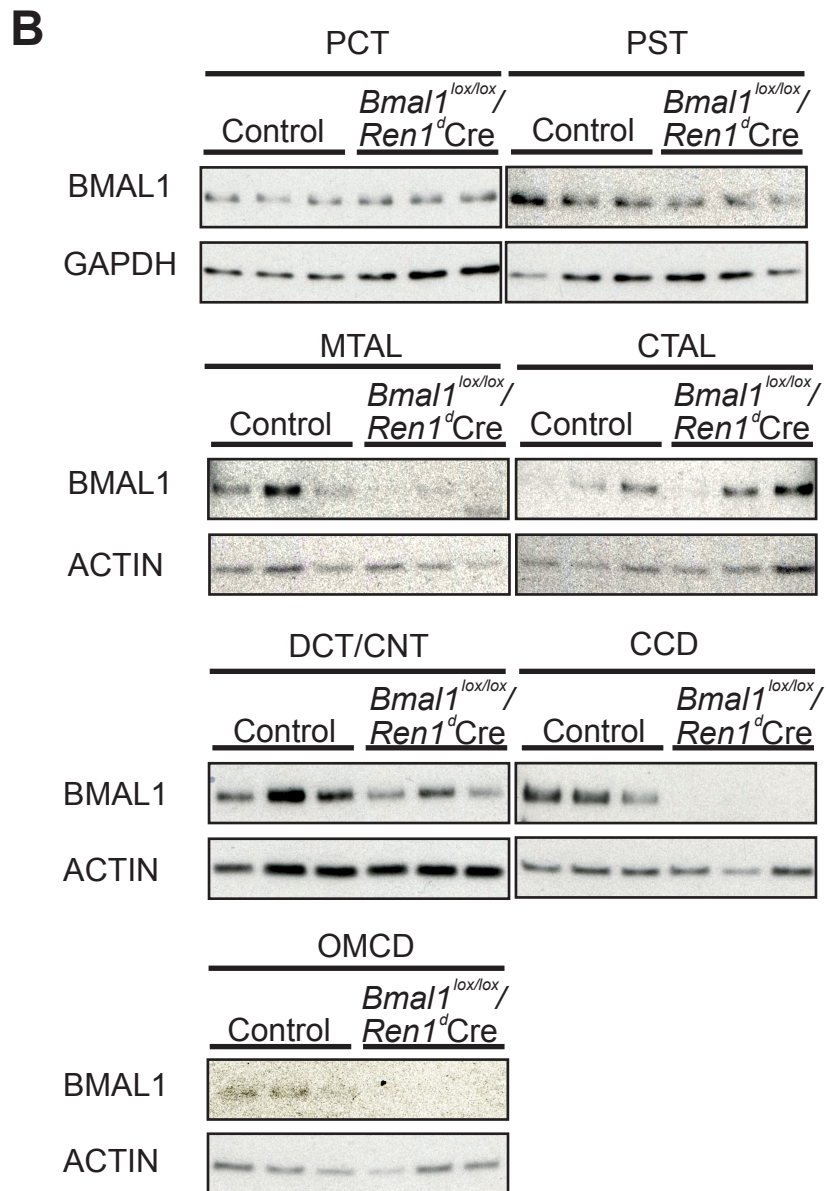
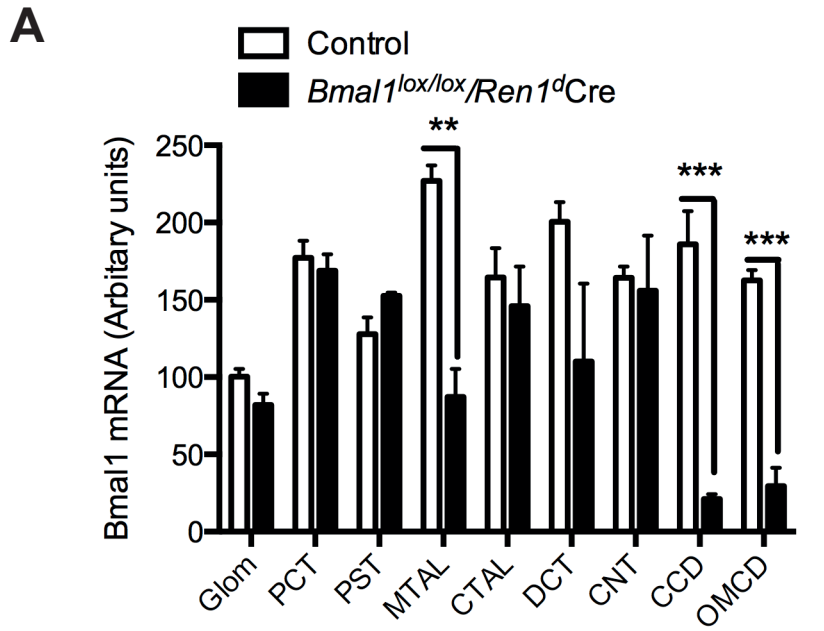


Figure 3, Tokonami et al.

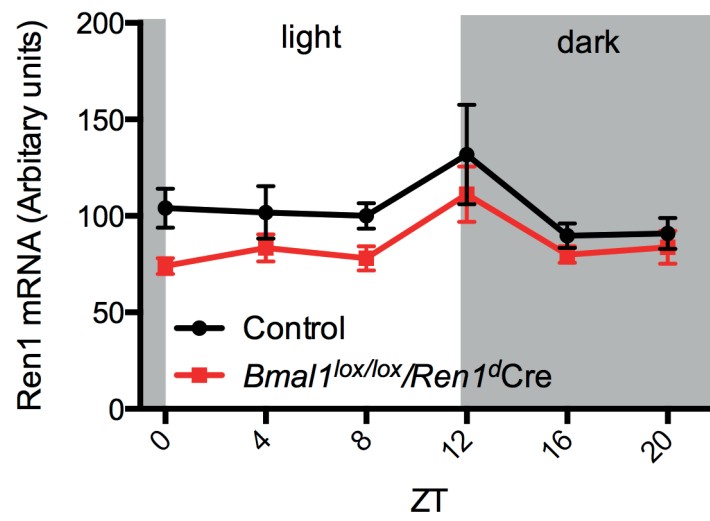
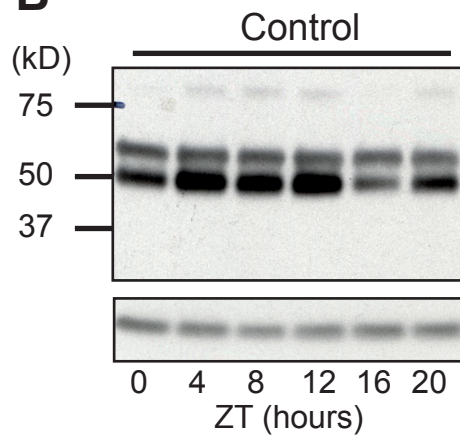
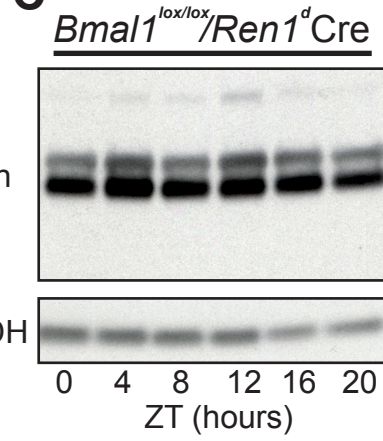
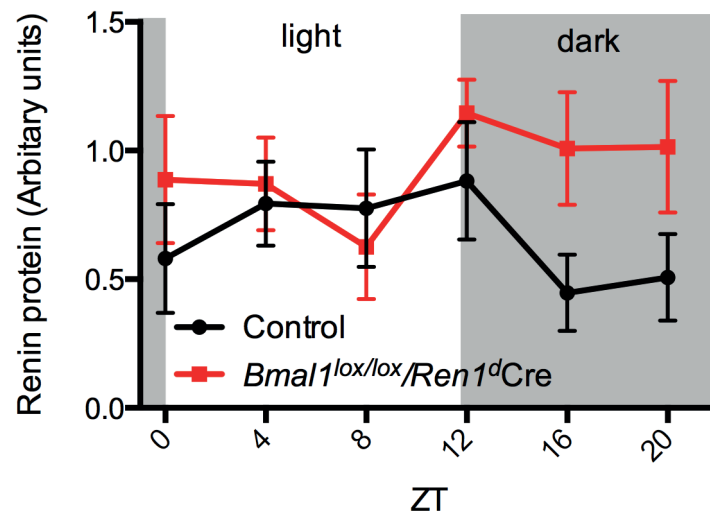
A**B****C****D**

Figure 4, Tokonami et al.

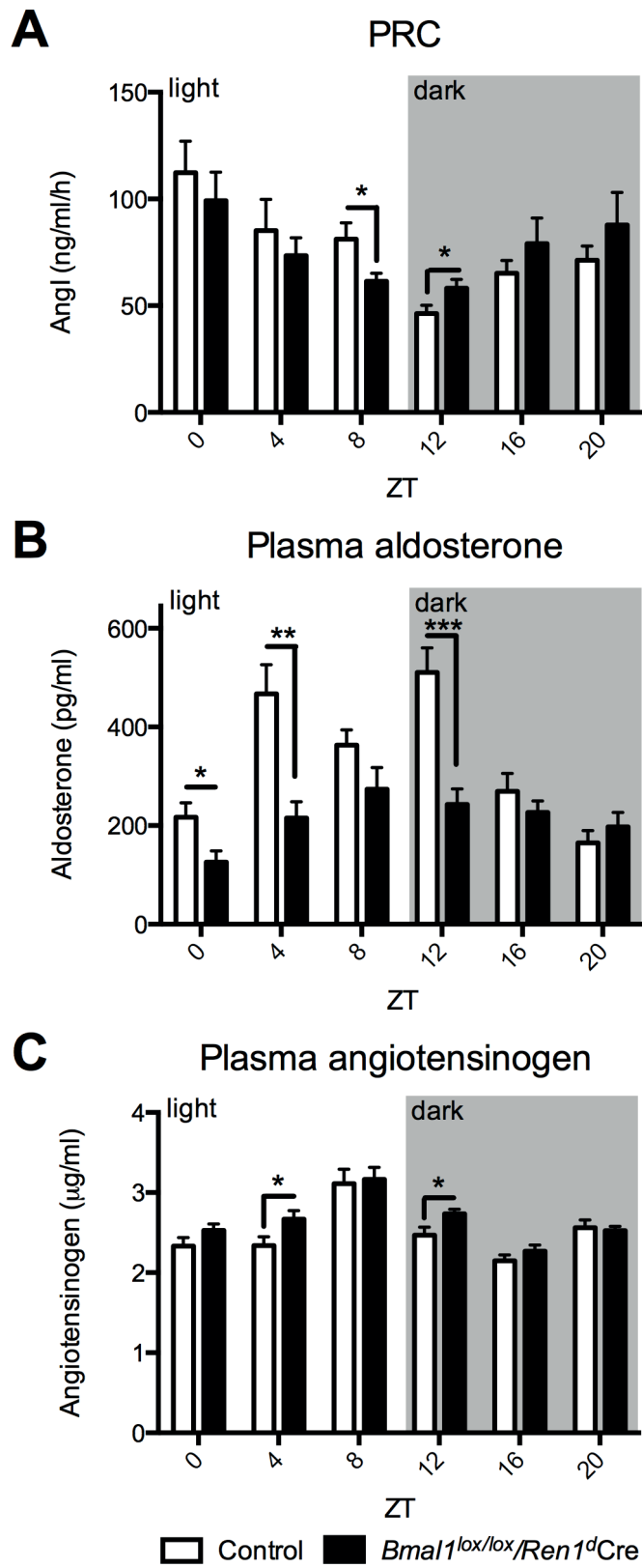
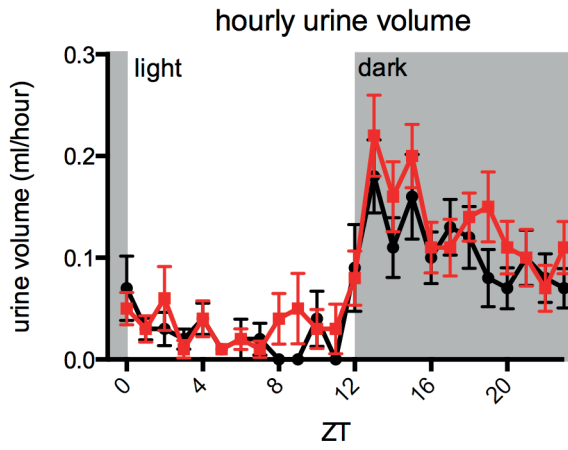
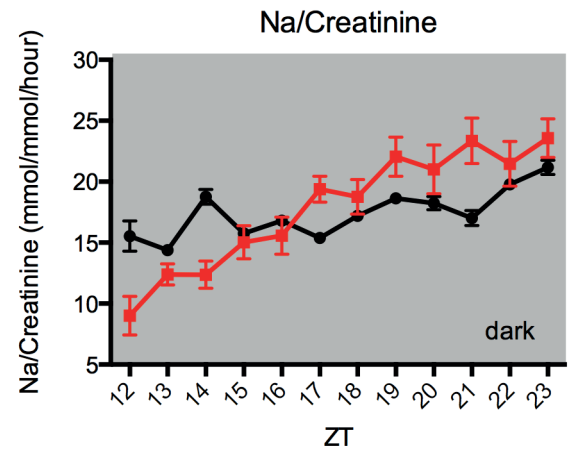
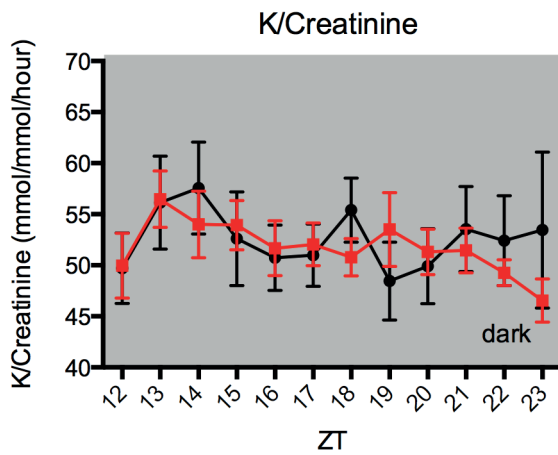
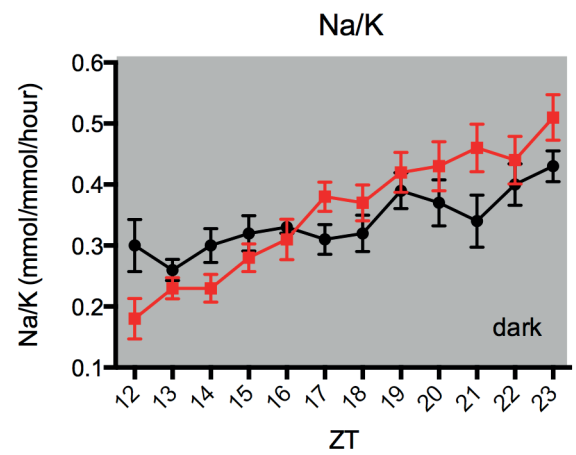


Figure 5, Tokonami et al.

A**B****C****D**

● Control

■ *Bmal1^{lox/lox}/Ren1^{dCre}*

Figure 6, Tokonami et al.

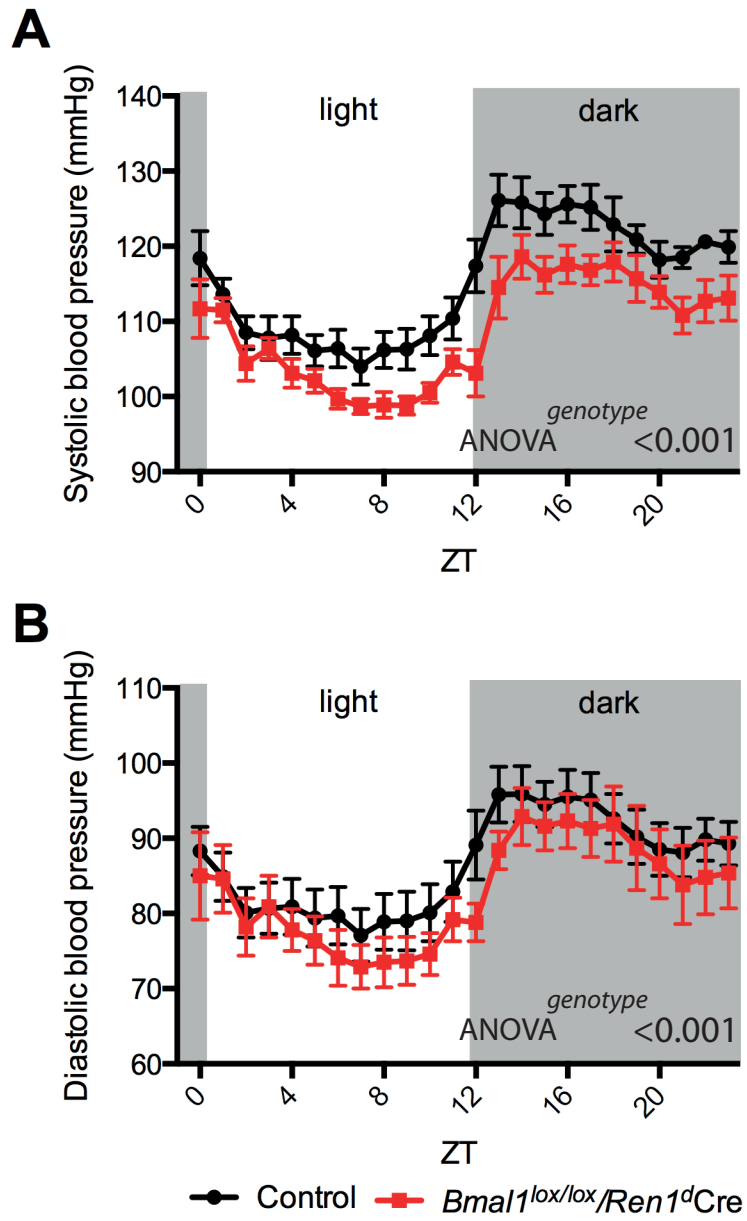


Figure 7, Tokonami et al.